

Theoretical and Numerical Studies of the Shell Equations of Bauer, Reiss and Keller, Part II: Numerical Computations

M. Hermann, D. Kaiser, M. Schröder

We study the solution field \mathcal{M} of a parameter-dependent nonlinear two-point boundary value problem suggested by Bauer et al. (1970). This problem models the buckling of a thin-walled spherical shell under a uniform axisymmetric external static pressure. In Part I (see Hermann et al., 1999) we have developed a mathematical theory which describes \mathcal{M} . In Part II of this work, the theoretical results are used to efficiently compute interesting parts of \mathcal{M} with numerical standard techniques.

1 Introduction

Let us consider the following parameter-dependent nonlinear two-point boundary value problem (BVP) which describes the buckling behavior of a thin-walled spherical shell under a uniform axisymmetric external static pressure

$$\begin{aligned} y_1'(t) &= (\nu - 1) \cot(t)y_1(t) + y_2(t) + [k \cot^2(t) - \lambda]y_4(t) + \cot(t)y_2(t)y_4(t) \\ y_2'(t) &= y_3(t) \\ y_3'(t) &= [\cot^2(t) - \nu]y_2(t) - \cot(t)y_3(t) - y_4(t) - 0.5 \cot(t)y_4^2(t) \\ y_4'(t) &= \beta y_1(t) - \nu \cot(t)y_4(t) \end{aligned} \quad 0 < t < \pi \quad (1)$$

$$y_2(0) = y_4(0) = y_2(\pi) = y_4(\pi) = 0 \quad (2)$$

where $y_1(t) = m(t)$, $y_2(t) = q(t)$, $y_3(t) = s(t)$ are proportional to the radial bending moment, the transversal shear and the circumferential membrane stress, respectively. The component $y_4(t)$ is proportional to the angle of rotation of a tangent to a meridian and ν is Poisson's ratio. Let the radii of the inner and outer surface of the spherical shell be given by $r = R \mp h$, where R is the radius of the midsurface of the shell and $2h$ is the uniform thickness. The parameter λ and the constants k, β are defined by

$$\lambda \equiv \frac{pR}{4Eh} \quad k \equiv \frac{1}{3} \left(\frac{h}{R} \right)^2 \quad \beta \equiv \frac{1 - \nu^2}{k}$$

where E is Young's modulus and p is a uniform compressive load. In the sequel we refer to λ as the load.

In Part I of this paper (see Hermann, Kaiser and Schröder, 1999) we developed a mathematical theory which describes the solution field \mathcal{M} of equations (1) and (2). We wrote the BVP as the second order problem

$$\begin{aligned} x_1''(t) &= -\cot(t)x_1'(t) + [\cot^2(t) - \nu]x_1(t) - x_2(t) - 0.5 \cot(t)x_2^2(t) \\ x_2''(t) &= -\cot(t)x_2'(t) + [\cot^2(t) + \nu]x_2(t) + \beta[x_1(t) - \lambda x_2(t) + \cot(t)x_1(t)x_2(t)] \end{aligned} \quad 0 < t < \pi \quad (3)$$

$$x_1(0) = x_2(0) = x_1(\pi) = x_2(\pi) = 0 \quad (4)$$

and transformed equations (3) and (4) into the operator equation

$$T(x, \lambda) = 0 \quad T : X \times \mathbb{R} \rightarrow Y \quad (5)$$

where X and Y are appropriate Banach spaces.

In Part II we show how this theory and appropriate numerical methods can be applied to compute interesting parts of \mathcal{M} . Our computations were based on $\nu = 0.32$ and $k = 10^{-5}$. The interval I_λ for the external load λ was set as $I_\lambda \equiv [0.005, 0.0077]$ because the primary bifurcation points $z_0 \equiv (0, \lambda_0)$ with the ten smallest λ -components are in $X \times I_\lambda$.

The organization of Part II is as follows: In Section 2, problem (3),(4) is transformed into a first order BVP on $[0, \pi/2]$ which can be solved by numerical standard software immediately. Moreover, relations describing the geometry of the deformed shells are given. In Section 3 we compute the simple bifurcation points and show how the jumping onto nontrivial solution branches can be realized. In Section 4, bifurcation diagrams of symmetric and nonsymmetric solutions are presented. The existence of secondary bifurcation points is proved numerically. Finally, in Section 5 we plot some deformed shells.

2 Numerical Approach

To determine an isolated solution $\bar{x} \in X$ of equation (5) for a fixed value $\bar{\lambda} \in I_\lambda$ we used the multiple shooting code RWPM (see e.g. Hermann and Kaiser, 1993,1994,1995) as the standard solver. Moreover, the software package RWPKV (see e.g. Hermann and Ullrich, 1992) was applied to trace the solution curves $\{(x(\varepsilon), \lambda(\varepsilon)) : |\varepsilon| \leq \varepsilon_0\}$ numerically. Both computer programs require the formulation of the BVP to be solved as a system of N first order differential equations and N two-point boundary conditions

$$\zeta'(t) = g(t, \zeta(t); \lambda) \quad a \leq t \leq b \quad r(\zeta(a), \zeta(b)) = 0 \quad (6)$$

Therefore, we transformed equation (5) into a BVP of the form (6) and removed the regular singularities of the differential equations as follows. Since the equivariance of the operator T (see Part I, equations (10) and (11)) implies $T(x, \lambda)(\pi - t) = -S_Y T(x, \lambda)(t) = -T(S_X x, \lambda)(t)$, the equation $T(x, \lambda)(t) = 0$, $t \in (0, \pi)$, can be split into the following two equations

$$T(x, \lambda)(t) = 0 \quad T(S_X x, \lambda)(t) = 0 \quad 0 < t \leq \pi/2 \quad x \in X \quad (7)$$

Defining the vector-valued function $\zeta(t) \equiv (\zeta_1(t), \dots, \zeta_8(t))^T$ by

$$\begin{aligned} \zeta_1(t) &\equiv x_1(t)/t & \zeta_2(t) &\equiv x'_1(t) & \zeta_3(t) &\equiv x_2(t)/t & \zeta_4(t) &\equiv x'_2(t) \\ \zeta_5(t) &\equiv (S_X x)_1(t)/t & \zeta_6(t) &\equiv (S_X x)'_1(t) & \zeta_7(t) &\equiv (S_X x)_2(t)/t & \zeta_8(t) &\equiv (S_X x)'_2(t) \end{aligned} \quad (8)$$

and using the splitting $\cot(t) = 1/t - \widehat{\cot}(t)$, $\widehat{\cot}(t) = O(t)$ for $t \rightarrow 0$, we transformed the equations (7) into the BVP of dimension $N=8$:

$$\zeta'(t) = \begin{cases} \frac{1}{t} M \zeta(t) + g(t, \zeta(t); \lambda) & 0 < t \leq \pi/2 \\ 0 & t = 0 \end{cases} \quad (9)$$

$$M \zeta(0) = 0 \quad \zeta_i(\pi/2) = -\zeta_{i+4}(\pi/2), \quad i = 1, 3 \quad \zeta_j(\pi/2) = \zeta_{j+4}(\pi/2), \quad j = 2, 4 \quad (10)$$

where

$$M = \text{diag}(M_1, M_1, M_1, M_1) \quad M_1 = \begin{pmatrix} -1 & 1 \\ 1 & -1 \end{pmatrix}$$

$$g_i(t, \zeta(t); \lambda) = 0 \quad i = 1, 3, 5, 7$$

$$\begin{aligned} g_2(t, \zeta(t); \lambda) &= -[2c\widehat{\cot}(t) - t(c\widehat{\cot}^2(t) - \nu)]\zeta_1(t) + c\widehat{\cot}(t)\zeta_2(t) - t\zeta_3(t) - \frac{t}{2}[1 - tc\widehat{\cot}(t)]\zeta_3^2(t) \\ g_4(t, \zeta(t); \lambda) &= -[2c\widehat{\cot}(t) - t(c\widehat{\cot}^2(t) + \nu)]\zeta_3(t) + c\widehat{\cot}(t)\zeta_4(t) \\ &\quad + \beta t\{\zeta_1(t) - \lambda\zeta_3(t) + [1 - tc\widehat{\cot}(t)]\zeta_1(t)\zeta_3(t)\} \\ g_6(t, \zeta(t); \lambda) &= -[2c\widehat{\cot}(t) - t(c\widehat{\cot}^2(t) - \nu)]\zeta_5(t) + c\widehat{\cot}(t)\zeta_6(t) - t\zeta_7(t) - \frac{t}{2}[1 - tc\widehat{\cot}(t)]\zeta_7^2(t) \\ g_8(t, \zeta(t); \lambda) &= -[2c\widehat{\cot}(t) - t(c\widehat{\cot}^2(t) + \nu)]\zeta_7(t) + c\widehat{\cot}(t)\zeta_8(t) \\ &\quad + \beta t\{\zeta_5(t) - \lambda\zeta_7(t) + [1 - tc\widehat{\cot}(t)]\zeta_5(t)\zeta_7(t)\} \end{aligned} \quad (11)$$

REMARK 1 The entry $\zeta'(0) = 0$ in formula (9) has been obtained by the following argument. Since $c\hat{o}t(t) = O(t)$ as $t \rightarrow 0$ and $M\zeta(0) = 0$, it follows

$$\zeta'(0) = \lim_{t \rightarrow 0^+} \zeta'(t) = \lim_{t \rightarrow 0^+} \left(M \frac{\zeta(t) - \zeta(0)}{t} + g(t, \zeta(t); \lambda) \right) = M\zeta'(0)$$

The eigenvalues of the matrix M are -2 and 0 (both with the multiplicity 4). Thus, the matrix $I - M$ is nonsingular and we compute $\zeta'(0) = 0$.

REMARK 2 For the determination of the symmetric solutions $(x_s, \lambda) \in X_s \times \mathbb{R}$ of equation (5) it is not necessary to use the whole system (9),(10). Since the relation $S_X x_s = x_s$ implies that the two equations in (7) are identical, only the first one has to be solved. This means that the transformed equations (9) can be reduced to

$$\begin{pmatrix} \zeta_1'(t) \\ \vdots \\ \zeta_4'(t) \end{pmatrix} = \frac{1}{t} \begin{pmatrix} M_1 & 0 \\ 0 & M_1 \end{pmatrix} \begin{pmatrix} \zeta_1(t) \\ \vdots \\ \zeta_4(t) \end{pmatrix} + \begin{pmatrix} g_1(t, \zeta_1(t), \dots, \zeta_4(t); \lambda) \\ \vdots \\ g_4(t, \zeta_1(t), \dots, \zeta_4(t); \lambda) \end{pmatrix} \quad (12)$$

The boundary conditions at $t = 0$ follow immediately from equations (10) whereas those at $t = \pi/2$ can be obtained from the fact that x_s is an odd function:

$$\zeta_1(0) = \zeta_2(0) \quad \zeta_3(0) = \zeta_4(0) \quad \zeta_1(\pi/2) = \zeta_3(\pi/2) = 0 \quad (13)$$

Obviously, the amount of computational work which is necessary to solve this BVP of dimension $N = 4$ is much smaller than that one to solve the problem (9),(10) of dimension $N = 8$.

In order to be able to visualize the computed deformed shells some further geometrical quantities are required (see also Bauer et al., 1970). Let us consider an arc $(R \sin(t), 0, R \cos(t)) \in \mathbb{R}^3$, $t \in [0, \pi]$, of the midsurface of the sphere which is deformed by the load λ to

$$(\tilde{R}(t) \sin(t + u(t)), 0, \tilde{R}(t) \cos(t + u(t))) \quad t \in [0, \pi] \quad (14)$$

where $\tilde{R}(t) \equiv R[1 - W_0 - w(t)]$ and $W_0 \equiv (1 - \nu)\lambda$. The quantities RW_0 and $Rw(t)$ are radial displacements. W_0 represents the uniformly contracted or unbuckled state whereas $w(t)$ describes the buckling of the shell. Suppose (x, λ) is a solution of equation (5). Then the functions u and w satisfy

$$\begin{aligned} u'(t) &= \cot(t)u(t) + (1 + \nu)[\cot(t)x_1(t) - x_1'(t)] - 0.5x_2^2(t) \\ w'(t) &= x_2(t) - u(t) \end{aligned} \quad (15)$$

$$0 = u(0) = u(\pi/2) = u(\pi) \quad w(\pi/2) = -x_1'(\pi/2) \quad (16)$$

Note that the condition for $w(\pi/2)$ in equation (16) has been obtained by adding the equations (A.19e) given in the article of Bauer et al. (1970), p. 567.

Now, the shape of the deformed shell can be computed as follows. The functions u and w determined from equations (15) and (16) are substituted into equation (14). Then this arc is rotated around the vertical axis which is spanned by the vector $(0, 0, 1)$. This yields the midsurface of the deformed shell. If (x, λ) is a symmetric solution of equation (5) then u and w are odd and even, respectively. Thus, a symmetric solution leads to a shell which is symmetrically deformed with respect to the equatorial plane.

3 Trivial Solution Curve

Consider the trivial solution curve $\mathcal{C}_{triv} \subset \mathcal{M}$. In engineering it is usual to denote the λ -component of a singular point as a critical value. To determine the critical values $\lambda_{0n} \in I_\lambda$ listed in Table 1 we used the explicit formula given in Part I, Theorem 3(1). The real numbers γ_n and the vectors $v_n \in \mathbb{R}^2$ are defined by $\gamma_n \equiv \beta/(\mu_n - 1 - \nu) + 1 + \nu$, and $A(\lambda_{0n})v_n = \mu_n v_n$, $v_n \neq 0$, respectively. It follows from Part I, Theorem 3(3) that $\dim \mathcal{N}(T_x(z_{0n})) = 2$ if and only if there exists an integer m with $\mu_m \equiv m(m+1) = \gamma_n$. Thus, γ_n is an indicator for the dimension of this null space. Looking at Table 1 we observe $\gamma_n \notin \mathbb{N}$, and consequently $\dim \mathcal{N}(T_x(z_{0n})) = 1$. The entries in the fourth column of Table 1 are justified by Part I, Theorem 2. Part I, Theorem 5 implies that all singular points z_{0n} given in Table 1 are simple bifurcation points. In other words, for each z_{0n} there is exactly one curve \mathcal{C}_n of nontrivial solutions which branches off at z_{0n} .

n	λ_{0n}	γ_n	basis of $\mathcal{N}(T_x(0, \lambda_{0n}))$
17	0.006683647223	295.9241749	$(P_{17}^1 \circ \cos)v_{17} \in X_a$
16	0.006717126563	332.9292803	$(P_{16}^1 \circ \cos)v_{16} \in X_s$
18	0.006737890528	264.7930539	$(P_{18}^1 \circ \cos)v_{18} \in X_s$
15	0.006855931104	377.3883761	$(P_{15}^1 \circ \cos)v_{15} \in X_a$
19	0.006866687913	238.3539073	$(P_{19}^1 \circ \cos)v_{19} \in X_a$
20	0.007060027591	215.7080768	$(P_{20}^1 \circ \cos)v_{20} \in X_s$
14	0.007124022503	431.4522599	$(P_{14}^1 \circ \cos)v_{14} \in X_s$
21	0.007310187241	196.1624069	$(P_{21}^1 \circ \cos)v_{21} \in X_a$
13	0.007554700365	498.1099048	$(P_{13}^1 \circ \cos)v_{13} \in X_a$
22	0.007611132736	179.1752746	$(P_{22}^1 \circ \cos)v_{22} \in X_s$

Table 1. Simple Bifurcation Points $z_{0n} \equiv (0, \lambda_{0n})$

To jump onto \mathcal{C}_n , i.e., to compute a point on the curve of nontrivial solutions we used a sophisticated trial and error procedure. The idea was to parametrize the curve \mathcal{C}_n in the form $x(\varepsilon) = \varepsilon\varphi_{0n} + w(\varepsilon)$, $\lambda(\varepsilon) = \lambda_{0n} + \tau(\varepsilon)$, where $\mathcal{N}(T_x(z_{0n})) = \text{span}\{\varphi_{0n}\}$, $w(\varepsilon)$ belongs to the complement of $\mathcal{N}(T_x(z_{0n}))$ in X and satisfies $w(\varepsilon) = O(\varepsilon^2)$, $\tau(\varepsilon) \in \mathbb{R}$ with $\tau(\varepsilon) = O(\varepsilon)$. Using the starting point $z^{(0)} \equiv (\varepsilon\varphi_{0n}, \lambda_{0n} + \tau)$, where $|\varepsilon|$ and $|\tau|$ are small, we tried to compute a solution of equation (5) with the code RWPM. Since RWPM requires a system of the form (9),(10) it was necessary to transform $z^{(0)}$ according to equation (8). By varying ε and τ we succeeded in jumping onto \mathcal{C}_n . Then, we applied the code RWPKV for tracing this curve.

With the theoretical results presented in Part I the computational work could be reduced as follows: Let n be odd (cf. Table 1). If z_{0n} is removed from the curve \mathcal{C}_n two solution branches Γ_1 and Γ_2 result. By Part I, Theorem 9(3) we know that all elements of Γ_1 are nonsymmetric. Therefore, it was sufficient to trace the branch Γ_1 only. After that, we determined the elements $(\bar{x}, \lambda) \in \Gamma_2$ from the elements $(x, \lambda) \in \Gamma_1$ by the formula $\bar{x} = S_X x$.

Now, let n be even. Looking at Table 1 we see that the one-dimensional null space $\mathcal{N}(T_x(z_{0n}))$ is a subset of X_s . By Part I, Theorem 9(1) we know that there is a sufficiently small neighbourhood $U \subset X \times \mathbb{R}$ of z_{0n} such that $\mathcal{C}_n \cap U \subset X_s \times \mathbb{R}$. As before, if z_{0n} is removed from the curve \mathcal{C}_n two solution branches Γ_1 and Γ_2 result. We have traced Γ_1 and Γ_2 on the basis of the BVP (12),(13). The use of this BVP is justified by Part I, Theorem 10 as long as we do not arrive at a singular point. Otherwise Part I, Theorem 9 gives the information how to continue.

4 Secondary Solution Curves

In the first bifurcation diagram of the symmetric solutions (see Figure 1) we represent a solution (x_s, λ) of equation (5) by the point $(\lambda, E(x_s, \lambda))$. The quantity $E(x, \lambda)$ is defined by

$$E(x, \lambda) \equiv \sqrt[3]{\frac{e(x, \lambda)}{2}} \cdot 10^3$$

where

$$e(x, \lambda) \equiv \int_0^\pi \left\{ (x_1')^2 + (\cot^2(t) - \nu)x_1^2 + \frac{(x_2' + \nu \cot(t)x_2)^2}{\beta} + k \cot^2(t)x_2^2 - 4\lambda w \right\} \sin(t) dt \quad (17)$$

This integral is proportional to the difference between the potential energy of a buckled solution (x, λ) and the unbuckled solution $(0, \lambda)$ (see Bauer et al., 1970).

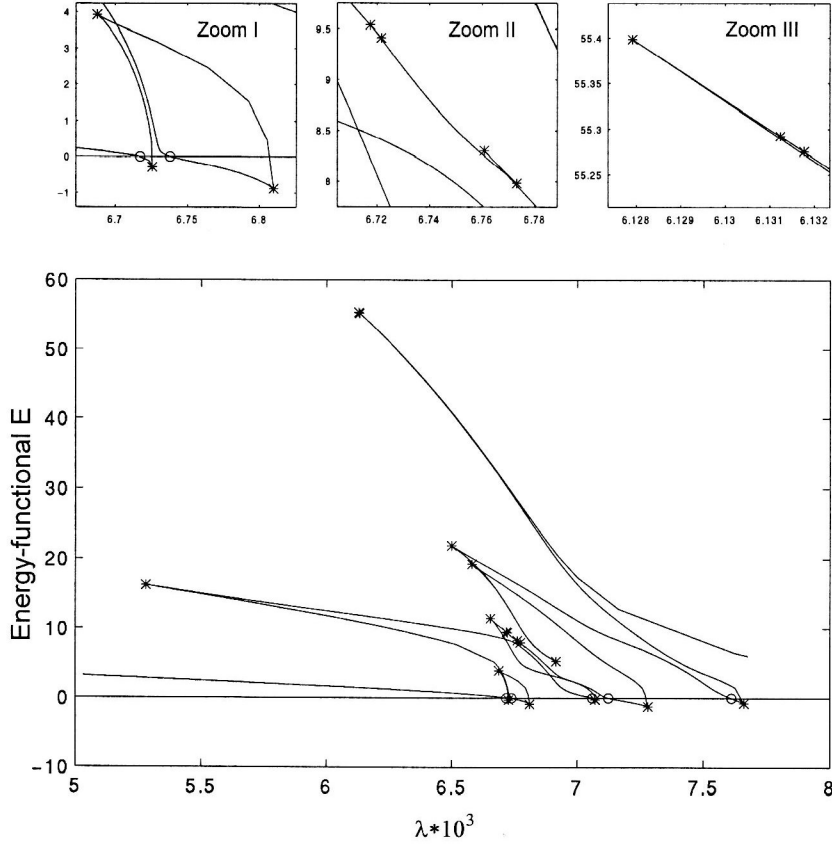


Figure 1. Bifurcation Diagram: Symmetric Solutions of Equation (5)
(o bifurcation points, * turning points)

During the pathfollowing of curves of symmetric solutions (n even) we have detected a number of turning points which are given in Table 2. The numerical techniques for the detection and computation of turning points implemented in RWPKV are described in the paper of Hermann and Ullrich (1992).

No.	$\lambda_0 \cdot 10^3$	$x'_{01}(0) \cdot 10^3$	$x'_{02}(0)$	E
1	6.7256022	0.3345044	0.0343114	-0.287
2	6.6873969	2.2078041	0.2356827	3.928
3	6.8100323	1.1683510	0.2990327	-0.892
4	5.2804210	5.1352283	-4.0172601	16.169
5	7.0711590	0.2834687	0.1484373	-0.226
6	6.6534707	-2.1610009	1.0663462	11.437
7	6.7215753	-5.0560232	-1.3052524	9.413
8	6.7174067	-5.2146032	-1.8304447	9.539
9	6.7732333	-4.1290496	-2.5178255	7.980
10	6.7607884	-4.6418851	-1.5797841	8.303
11	7.2822908	1.5762264	0.2966017	-1.262
12	6.5807714	2.9035722	-0.0308069	19.242
13	6.9156469	9.4104e-4	-0.9309247	5.278
14	6.4991517	3.8449160	-4.3006411	21.883
15	7.6601766	0.9855033	0.4261658	-0.743
16	6.1279061	-4.3589349	0.9343079	55.399
17	6.1317663	-5.8035606	0.3040023	55.275
18	6.1312388	-6.3622172	-0.0092440	55.292

Table 2. Symmetric Case: Turning Points $z_0 \equiv (x_0, \lambda_0)$

In Figure 2 the computed symmetric solutions are marked with dots in order to visualize the stepsize strategy used in the pathfollowing code RWPKV. Moreover, in this picture we have used the functional $x'_1(0)$ instead of E . By this change another insight into the structure of the solution field is obtained.

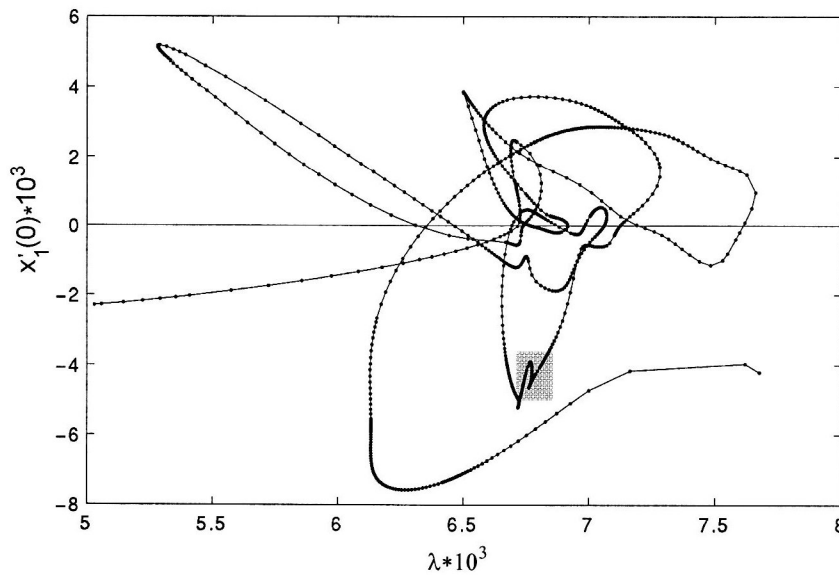


Figure 2. Bifurcation Diagram: Symmetric Solutions of Equation (5)

Since $e(x, \lambda) = e(S_X x, \lambda)$, the functional (17) is not suitable to represent nonsymmetric solutions in a bifurcation diagram. Therefore we have only plotted $x'_1(0)$ versus λ in case of the nonsymmetric solutions (see Figure 3).

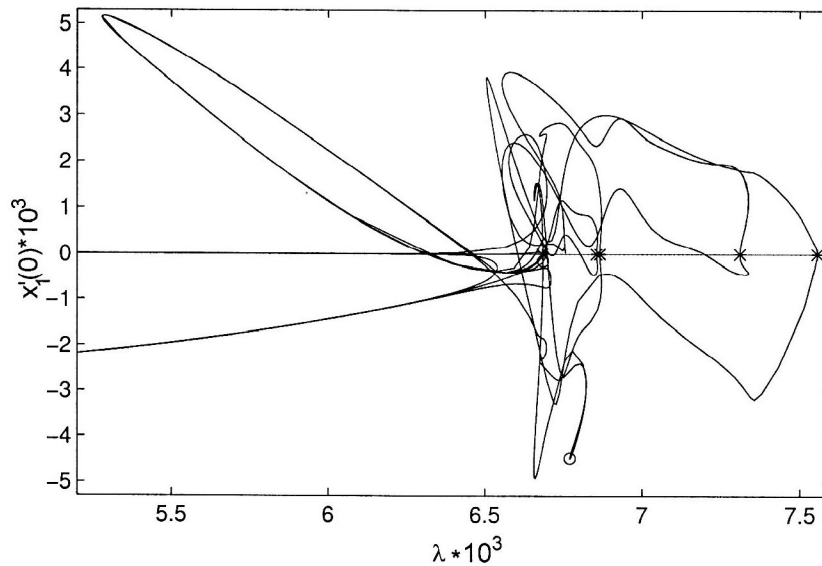


Figure 3. Bifurcation Diagram: Nonsymmetric Solutions of Equation (5)

To gain a better insight into the structure of the solution field the curves of nonsymmetric solutions which pass through the bifurcation points $(0, \lambda_{0n})$, $n = 13, 15, 17, 19, 21$, are drawn in Figure 4(a)-4(e)

separately. Moreover a curve which passes through a secondary bifurcation point is drawn in Figure 4(f).

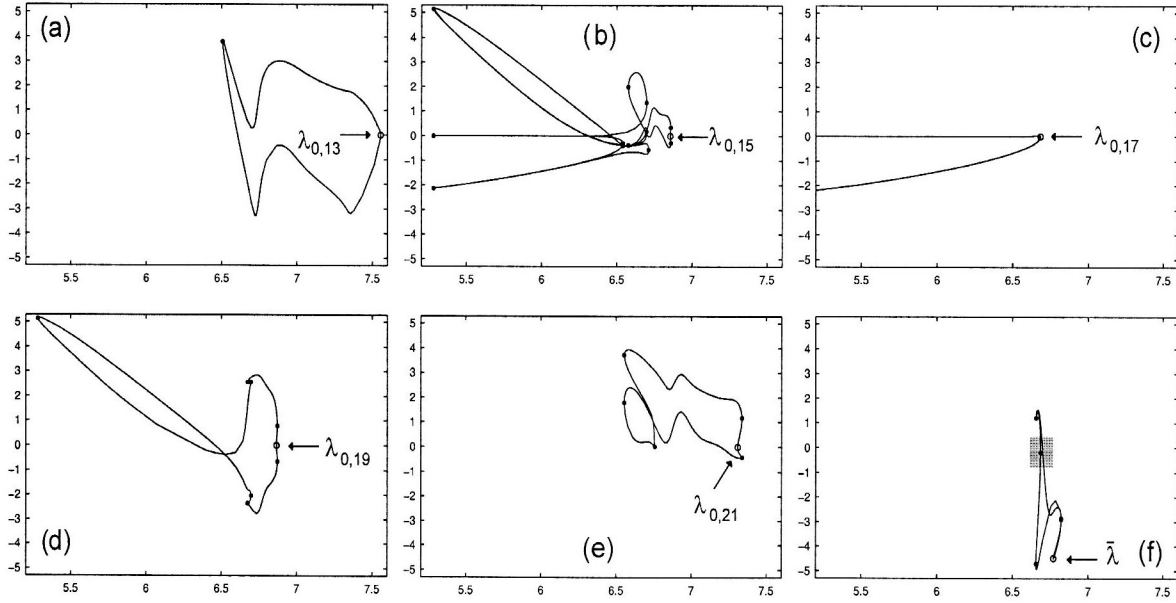


Figure 4. Curves of Nonsymmetric Solutions of Equation (5)
Note: ● - turning point, ○ - bifurcation point

In Table 3 the turning points of the curves of nonsymmetric solutions drawn in Figure 4 are given. They have been determined in the same way as the turning points of the curves of symmetric solutions.

Picture in Figure 4	$\lambda_0 * 10^3$	$x'_{01}(0) * 10^3$	$x'_{02}(0)$	$\lambda_0 * 10^3$	$x'_{01}(0) * 10^3$	$x'_{02}(0)$
(a)	6.5046598	3.7920602	-4.3823691			
(b)	6.8588862	0.3511653	0.0526280	6.8588862	-0.2847266	-0.0316046
	6.5758915	-0.3769640	-1.5335074	6.5758915	1.9929949	0.9526770
	6.6981940	0.1737112	-0.5577584	6.6981940	1.3595862	0.1347339
	5.2803832	5.1340731	-4.0167780	5.2803832	5.3830e-6	3.2214e-6
	6.5396708	-0.3915986	-4.0493111	6.5396708	-2.9800398	-0.1004188
	5.2803827	5.1340741	-4.0167778	5.2803827	-2.1331971	-1.0566922
	6.7111445	-0.5583289	-0.7491602			
(c)	no turning points with $\lambda \in I_\lambda$					
(d)	6.8718367	0.7839775	0.2181021	6.8718367	-0.6474939	-0.2473561
	6.6745882	2.5563482	0.2609639	6.6745882	-2.3458582	-2.8146447
	6.6973295	2.5674983	0.3234533	6.6973295	-2.0401186	-3.4150051
	5.2804352	5.1370983	-4.0179866			
(e)	7.3377969	1.1712018	0.4100209	7.3377969	-0.4079664	-0.3783673
	6.5541909	3.7167771	0.3988890	6.5541909	1.7947468	-3.4242751
	6.7574505	0.0236994	-1.8623094			
(f)	6.8239872	-2.9090798	-3.1205232	6.8239872	-2.8575320	-0.0511785
	6.6562690	-4.7021856	-0.7175737	6.6562690	1.2117335	1.5324841
	6.6855269	-0.1499650	1.3752581			

Table 3. Nonsymmetric Case: Turning Points $z_0 \equiv (x_0, \lambda_0)$

In order to demonstrate the existence of secondary bifurcation points of equation (5) we have executed the pathfollowing process in the grey shaded area of Figure 2 with the large system (9) to (11) instead of the reduced system (12),(13). The result is represented in Figure 5.

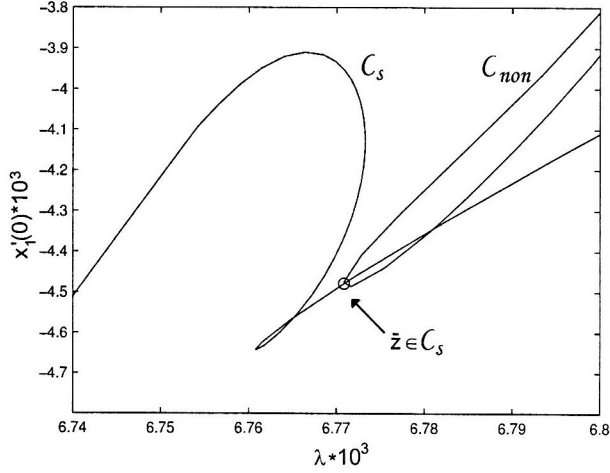


Figure 5. Secondary Bifurcation Point of Equation (5)

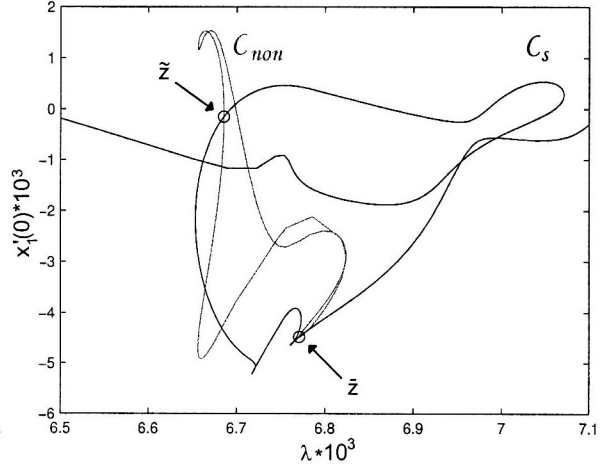


Figure 6. Part of $\tilde{C}_s = C_s$ with Two Secondary Bifurcation Points

We see that the point $\bar{z} = (\bar{x}, \bar{\lambda}) \in C_s \subseteq X_s \times \mathbb{R}$ is a candidate for a secondary bifurcation point. Let us assume that the curve of nonsymmetric solutions C_{non} intersects C_s at \bar{z} . Part I, Theorem 9(1) implies the existence of an antisymmetric element $\varphi_a \neq 0$ such that $T_x(\bar{z})\varphi_a = 0$. We have tried to compute this singularity with the well-known extended system (see e.g. Wallisch and Hermann, 1987)

$$T(x_s, \lambda) = 0 \quad T_x(x_s, \lambda)\varphi_a = 0 \quad \varphi_a^* \varphi_a = 1 \quad (18)$$

Note that the first equation of (18) corresponds to the system (12),(13). Because of the symmetry of x_s , the antisymmetry of φ_a and the equivariance of T it is sufficient to solve $[T_x(x_s, \lambda)\varphi_a](t) = 0$ on the smaller interval $(0, \pi/2]$. We transformed φ_a analogously to x_s (see equations (8)) and obtained a system of differential equations which is of the form (12), with modified functions g_i . Then, we determined the corresponding boundary conditions at $t = \pi/2$ from the relation $\varphi_a'(\pi/2) = 0$. The nonlinear two-point boundary value problem which results from equations (18) by these manipulations consists of 10 differential equations (including the trivial differential equation $\lambda' = 0$) and 10 boundary conditions. After 18 iterations the code RWPM produced the solution

$$(\bar{x}'_1(0), \bar{x}'_2(0), \bar{\lambda}) = (-0.004478227, -1.258771, 0.006770837)$$

From the pathfollowing process for C_s we know that \bar{z} cannot be a turning point of C_s . Thus \bar{z} is indeed a secondary bifurcation point.

Part I, Theorem 11 can also be applied to determine secondary bifurcation points. In the grey shaded area of Figure 4 we find the situation which is assumed in this theorem. Let us denote the marked point by $\tilde{z} \equiv (\tilde{x}, \tilde{\lambda})$. Then we have $\tilde{z} = (x(\varepsilon_0), \lambda(\varepsilon_0)) \in X_s \times \mathbb{R}$. Part I, Theorem 11 states that there is an element $\varphi_a \in X_a \setminus \{0\}$ such that $T_x(\tilde{z})\varphi_a = 0$. We determined (\tilde{z}, φ_a) by the extended system (18) restricted to $t \in (0, \pi/2]$ and obtained

$$(\tilde{x}'_1(0), \tilde{x}'_2(0), \tilde{\lambda}) = (-1.499650 e-4, 1.375258, 0.006685527)$$

Then we assumed $\dim \mathcal{N}(T_x(\tilde{z})) = 1$, i.e., $\mathcal{N}(T_x(\tilde{z})) = \text{span}\{\varphi_a\}$. Consequently, \tilde{z} is an isolated solution of $T|_{X_s \times \mathbb{R}}(z_s) = 0$. The implicit function theorem yields a uniquely determined curve of symmetric solutions

$$\tilde{C}_s = \{z(\lambda) = (x(\lambda), \lambda - \tilde{\lambda}) : |\lambda| < \lambda_0\} \quad z(0) = \tilde{z}$$

Starting in \tilde{z} we applied the pathfollowing procedure to the reduced system for symmetric solutions (12),(13), first into the positive λ -direction then into the negative one. In this way we determined \tilde{C}_s (see Figure 6). Thus, there are two branches of nonsymmetric solutions which branch off from \tilde{C}_s at \tilde{z} , i.e., \tilde{z} is a secondary bifurcation point. Obviously, $\tilde{C}_s = C_s$.

5 Examples of Deformed Shells

Finally, let us present some examples of deformed shells. We computed the arc (14) at 201 equidistributed points $t_i = i\pi/200, i = 0, \dots, 200$. Then, this discretized object was reproduced for each $\alpha_j = j\pi/200, j = 1, \dots, 400$, where α_j denotes the angle of rotation around the vertical axis. By this strategy we obtained a discretization of the midsurface of the shell which was interpolated and drawn with the mathematical software package MATLAB (see e.g. Pärt-Enander et al., 1996).

Let z_1 and z_2 be a pair of nonsymmetric solutions of equation (5) and S_1, S_2 the corresponding deformed shells. In Figure 7(d) we have drawn the left part of S_1 and the right part of S_2 . By this procedure the nonsymmetry of the deformed shell can be better recognized.

The symmetric deformed shells (a)-(c) of Figure 7 correspond to solutions (x, λ) which are plotted in Figure 1. The two nonsymmetric deformed shells shown in picture (d) can be seen in Figure 4(e) (here, $x'_1(0) = 1.6989288 \text{ e-}3, (S_X x)_1'(0) = 3.6697240 \text{ e-}3$).

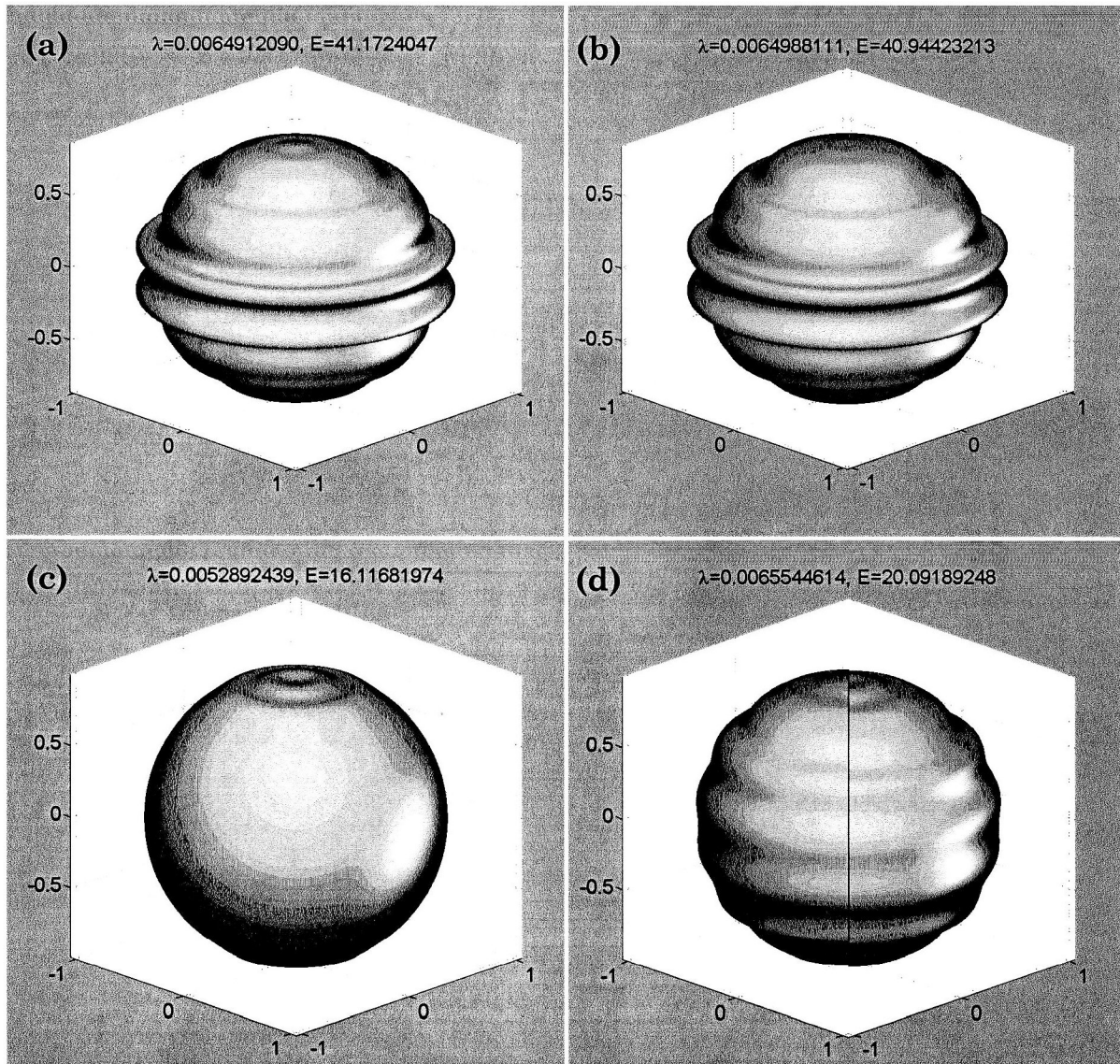


Figure 7. Examples for Deformed Shells: (a)-(c) Symmetric Solutions, (d) Representation of a Pair of Nonsymmetric Solutions

Acknowledgements. This research was supported by the Thuringian Ministry of Science, Research and Culture under Grant B501-96076.

Literature

1. Bauer, L.; Reiss, E. L.; Keller, H. B.: Axisymmetric buckling of hollow spheres and hemispheres. *Communications on Pure and Applied Mathematics*, 23, (1970), 529–568.
2. Hermann, M.; Kaiser, D.: RWPM: a software package of shooting methods for nonlinear two-point boundary value problems. *Appl. Numer. Math.*, 13, (1993), 103–108.
3. Hermann, M.; Kaiser, D.: RWPM: a software package of shooting methods for nonlinear two-point boundary value problems, documents and programs, (1994). (anonymous ftp: ftp3.mathe.uni-jena.de/pub/mathe/RWPM/DOS).
4. Hermann, M.; Kaiser, D.: Shooting methods for two-point BVPs with partially separated endconditions. *ZAMM*, (1995), 651–668.
5. Hermann, M.; Kaiser, D.; Schröder, M.: Theoretical and numerical studies of the shell equations of Bauer, Reiss and Keller, Part I: Mathematical Theory. *Technische Mechanik*, Band 19, Heft 1, (1999), 53–62.
6. Hermann, M.; Ullrich, K.: RWPKV: a software package for continuation and bifurcation problems in two-point boundary value problems. *Appl. Math. Letters*, 5, (1992), 57–62.
7. Pärt-Enander, E.; Sjöberg, A.; Melin, B.; Isaksson, P.: *The MATLAB Handbook*. Addison-Wesley, Harlow et al., (1996).
8. Wallisch, W.; Hermann, M.: *Numerische Behandlung von Fortsetzungs- und Bifurkationsproblemen bei Randwertaufgaben*. Teubner-Texte zur Mathematik, Bd. 102, Teubner Verlag, Leipzig, (1987).

Address: Professor Dr. M. Hermann, Dr. D. Kaiser, Dipl.-Math. M. Schröder, Friedrich-Schiller-Universität, Institut für Angewandte Mathematik, Ernst-Abbe-Platz 1–4, D-07740 Jena, Germany